AUTHOR(S): TOKODE, O., PRABHU, R., LAWTON, L.A. and ROBERTSON, P.K.J.

TITLE: A photocatalytic impeller reactor for gas phase heterogeneous photocatalysis.

YEAR: 2017

Publisher citation: TOKODE, O., PRABHU, R., LAWTON, L.A. and ROBERTSON, P.K.J. 2017. A photocatalytic impeller reactor for gas phase heterogeneous photocatalysis. Journal of environmental chemical engineering [online], 5(4), pages 3942-3948. Available from: https://doi.org/10.1016/j.jece.2017.07.068

OpenAIR citation: TOKODE, O., PRABHU, R., LAWTON, L.A. and ROBERTSON, P.K.J. 2017. A photocatalytic impeller reactor for gas phase heterogeneous photocatalysis. Journal of environmental chemical engineering, 5(4), pages 3942-3948. Held on OpenAIR [online]. Available from: https://openair.rgu.ac.uk

A photocatalytic impeller reactor for gas phase heterogeneous photocatalysis

Oluwatosin Tokode[a*], Radhakrishna Prabhu[b], Linda A Lawton[c] and Peter K. J. Robertson[d]

[a]Department of Engineering, Coventry University Coventry, CV1 5FB United Kingdom.

[b]School of Engineering, Sir Ian Wood Building, Robert Gordon University Aberdeen, AB10 7GJ, United Kingdom.

[c]School of Pharmacy and Life sciences, Sir Ian Wood Building Robert Gordon University, Garthdee Road, Aberdeen AB10 7GJ, United Kingdom.

[d]School of Chemistry and Chemical Engineering, Queen's University Belfast, David Keir Building, Stranmillis Road, Belfast BT9 5AG, United Kingdom.

Abstract

A novel photocatalytic reactor based on a stirred tank configuration has been described. This reactor employs the use of photocatalytic impellers to aid the mass transport of gaseous organic compounds during photocatalytic reactions. Experiments involving toluene vapour photo-oxidation showed the reactor configuration is susceptible to catalyst deactivation even at low concentrations if treated for prolonged periods. For this reactor, the reactive time scale exceeds the diffusive time scale hence, toluene photo-oxidation was reaction limited. The dependency of photonic efficiency of the reaction on mass transfer and catalyst deactivation was observed when correlated with the Damköhler number and deactivation induced reduction reaction rates respectively. The results show an inverse variation with Damköhler number and proportionality to reaction rates.

Keywords

Titanium dioxide, Thin film, Reactor engineering, Photocatalysis, Catalyst deactivation

*Corresponding Author

E-mail: olu.tokode@cuc.coventry.ac.uk Tel: +44 02477659684

1. Introduction

Heterogeneous photocatalysis using semiconductor catalysts is an advanced oxidation process[1,2] with environmental applications in air remediation[3], hydrogen generation[4], corrosion prevention[5] and water purification[6-9]. Its application in environmental remediation is of significant importance because of its capability for complete degradation of organic and inorganic hazardous compounds[10,11]. The process is initiated when the catalyst particle absorbs photons having energy equal to or greater than the bandgap of the semiconductor catalysts. Upon band gap excitation, highly reactive holes (h^+) and electrons (e^-) are generated, these two go on to generate highly oxidizing hydroxyl radical ($OH^\bullet$) and reductive superoxide (O^-_2)[10,12,13]. The photo-generated species take part in redox reactions either on the surface or in the bulk with a characteristic low efficiency because of the recombination of electrons and holes. Heterogeneous photocatalytic reactions require the adequate interaction of photons, semiconductor catalyst and the pollutant molecule to achieve complete degradation of pollutants. As a result, special attention must be paid to the design of photocatalytic reactors to facilitate these processes. In recent years, there have been a concentration of efforts on the synthesis of highly active titanium dioxide catalysts[14-17] and more importantly, design of reactors for heterogeneous photocatalysis. This has led to different reactor configurations being reported in the research literature[18-21].

Photocatalytic reactors in heterogeneous photocatalysis bring together all components required for the photocatalytic reaction process to take place. These components such as photons, pollutant and catalyst that are required for the transformations of reactants interact when brought together into a single unit. Their interactions in a single unit reactor enables the monitoring and/or regulation of parameters such as mass transfer, temperature and concentration. This ensures that photons are adequately utilized, intermediate products can be identified and kinetics of the photocatalytic process can be studied. Therefore, the aim of reactor design is to optimize these elements and parameters to neutralise the pollutant

completely and achieve the greatest possible yield. In order to achieve this, a large catalyst surface area is essential. Catalysts in the powdered form provide a larger surface area than immobilized catalysts which have significantly reduced surface area. The use of immobilized catalysts has however, now been widely reported in the literature[22] because it eliminates the cost of separating powdered catalysts from liquid in solid-liquid treatment processes. They also provide numerous reactor design possibilities in gas-solid treatment. Different reactor configurations exist for gas-solid heterogeneous photocatalysis; Cassano and Alfano[23] identified the four most widely reported configurations in the photocatalytic literature to be monoliths[24], packed bed[25], catalytic walls[26] and fluidised bed[27] reactors. Previous studies employing these reactor configurations failed to bring together all reactor components required for transformations of reactants into a single unit. Li Puma and Yue[28] used a pilot plant falling film reactor to compare effectiveness of photon-based oxidation processes. The reactor was designed for optimal light absorption however, the feed tank which supplied the pollutant and the collector tank which collects treated fluids were external to the reaction chamber which housed the UV lamp. Adams *et al.*[29] designed a single pass, continuous flow drum reactor for wastewater treatment. The reactor employed three separate but connected drum reactors with paddles positioned on the inside of the reactor drum to allow the mixing of wastewater with catalysts pellets. UV lamps were in each drum to illuminate the catalyst. Residence time in each drum was 3 minutes hence, three drums were required to increase the overall residence time and consequently, the treatment time of pollutants. This led to a separation of the reactor unit into sub-units. For slurry reactors where the catalyst is a separate unit within the reactor, mass transfer limitations are not of great concern. Martin *et al.*[30] however, reported a decrease in reactor efficiency at high catalyst loading. This was as a result of restrictions in radiation transport when optical thickness of the catalyst suspension exceeded the optimum level. Fluidised bed reactors use an upward air stream to bring powdered catalysts into contact with gas phase pollutants suffer a similar limitation. Kuo *et al.*[31] reported the limitations of fluidised bed reactors to include powdered catalyst drifting away from the main reaction area of the reactor. This is due to the powdered catalyst

being a separate unit within the reactor. The fine structure of the TiO_2 powder may also lead to losses through trapping of the powder in reactor crevices.

The immobilized reactor configuration has been reported to be effective in providing adequate interaction between photons, catalyst and pollutant within the reactor. The supports on which these catalysts are immobilized vary greatly. Supports reported in the literature include but are not limited to glass, silica and optical fibre[22]. An ideal support should exhibit strong affinity for the pollutants, high specific surface area and strong binding with the catalyst without reduction in catalyst activity. Peill and Hoffmann[32] reported the design of an optical fibre reactor (OFR) which employed optical fibre cables as a means of light transmission to the catalyst. The TiO_2 catalyst was immobilised on the fibre cores. UV illumination from an external lamp was transmitted through the optical fibre into the reaction chamber hence, pollutant, photons and catalyst were a single unit in the reactor. The OFR reactor configuration reduced mass transport limitations however, stiffer fibres with separators were recommended to prevent delamination of the catalyst coating. In immobilized photoreactor development, the major challenges encountered are complications of reactor scale-up such as mixing, mass transport, reactant-catalyst contact and installation of catalysts and achieving a high ratio of activated catalyst to illuminated surface through efficient light intensity distribution inside the reactor[33]. These challenges can be adequately addressed through innovative reactor design using design concepts from various reactor configurations.

In this study, the development of a photocatalytic impeller reactor (PIR) for gas phase photocatalysis with a potential to overcome the aforementioned challenges is reported. This is the first heterogeneous photocatalysis study in the gas phase to investigate the use of the PIR reactor configuration. It is designed to have the catalyst, UV source, reactor chamber and mixing impellers as a single unit while overcoming mass transport limitations of an immobilised catalyst. The catalyst was supported on modified rushton impellers to make them photoactive and improve

reactant-catalyst contact. This reactor configuration's potential to overcome mass transport limitations by the mixing action of the impellers while under constant illumination by a UV LED array surrounding the reaction chamber was evaluated. Toluene vapour was used as a model pollutant and its photo-oxidation was used to evaluate the reactor performance.

2. Materials and methods

2.1 Immobilized TiO_2 catalyst preparation

Titania sol-gel was synthesized through the polymeric route[34] using a titanium tetraisopropoxide (TTIP, Sigma Aldrich) precursor. 5 mL of TTIP was added to 65 mL of 2-propanol (Fisher) and stirred vigorously for 2 hours. Subsequently, a mixture of 51 µL of 15.7 M nitric acid, 349 µL distilled water and 5 mL 2-propanol was added dropwise and stirred for 15 minutes. The resulting titania sol-gel was sonicated for 2 minutes and left standing for 24 hours. Thick layers of TiO_2 were immobilized on glass slides (38×12×6 mm, Fisher) by dip coating, the glass slides were wholly submerged in the sol-gel for 60 seconds and slowly withdrawn. The coated slides were allowed to air dry for an hour before undergoing heat treatment in a furnace at 500°C for an hour.

2.2 Photocatalytic Impeller Reactor (PIR)

The photocatalytic impeller reactor (PIR) is a gas phase reactor which operates in principle as a stirred tank reactor. The reactor system consists of an ultra-band UV LED (FoxUV™) array. Each UV LED was 5 mm round with wavelength peak at 360 nm, viewing angle of 15° and typical radiant power maintenance of >90% past 1200 hours. The UV LED array was wrapped around the reaction chamber as the illumination source. The reaction chamber was made of a transparent PMMA tubing (Plexiglas® XT) with 92% UV transmission hence, virtually all UV irradiation from the light source is incident in the reaction chamber. A vertically aligned stainless steel (316) shaft running through the centre of the chamber supports the impellers in the reactor. The impellers consist of glass slides (Fisherbrand FB58620) coated with TiO_2 and the coated slides are inclined at 30° and arranged perpendicularly to each other on circular discs. The immobilized

TiO_2 film makes the impellers photoactive. A schematic of the designed reactor is shown in figure 1.

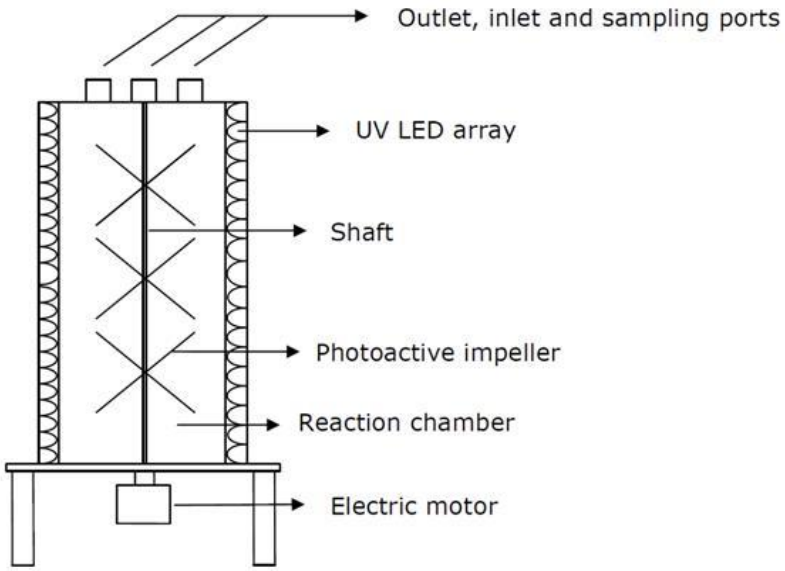

Figure 1. Schematic of photocatalytic impeller reactor

The shaft is supported at the top and bottom by ball bearings which make its rotation possible and sealed at the bottom with a double lip Viton rubber shaft seal where it exits the chamber and connects to a reversible synchronous motor (Crouzet). The reactor is sealed at the bottom with Viton gaskets as well as the top where three ports are located. The ports are an outlet sealed with propylene 2-way ball valves having Viton seals, an inert septum sealed inlet and a sampling port fitted with a filter and valve.

2.3 Experimental operating conditions

The PIR reactor was operated in batch mode, the inlet and outlet were sealed during operation while sampling took place through the sampling port. This ensured there was no channelling effect. All toluene photo-oxidation reactions were carried out at a temperature of 23 °C, at atmospheric pressure. The reaction chamber of the reactor had an effective volume of 1.4 L with the immobilised catalyst having a total surface area of 0.025 m^2. The starting concentration of toluene in the reactor was 11 ppm due to the small total surface are of the immobilised catalyst. An array of UV LEDs characterized in our lab to have an average radiant power of 435

μW each illuminated the reaction chamber. The UV LED array produced an incident photon rate of 3.03×10^{17} photons per seconds under continuous illumination.

3. Results

3.1 Mass transfer in the PIR reactor

Generally for immobilized reactors, the surface area of the catalyst is greatly reduced therefore, reactants travel longer distances before reaching photocatalytically active sites. This results in mass transfer limitations in immobilized reactors[35]. Mass transfer is driven by a gradient in chemical potential or convection forces within reactors. In the photocatalytic impeller reactor, it is aided by the rotating motion of the photocatalytic modified rushton impellers which provide a radial flow of the gas within the reactor. Figure 2 shows a flow field simulation within the reactor during operation using the RNG k-ε turbulence model. The RNG k-ε model is derived from the instantaneous Navier-Stokes equations using the renormalisation group theory mathematical technique. The model is more reliable for a wider class of flows when compared with both the Realisable k-ε and the Standard k-ε which are the other k-ε turbulence models. It offers improved accuracy in enclosed rotating flows hence, it is suitable for accounting for the effects of the small scales of motion within the PIR reactor.

In a photocatalytic impeller reactor with single pollutant molecule, rapid mixing is not the objective but the elimination of concentration gradients. For this reactor design, this is achieved with three 4-bladed impellers of equal clearance. The rotating impellers distribute the turbulence uniformly, creating separate zones while reducing areas with little or no kinetic energy as a result of the flow.

(a)

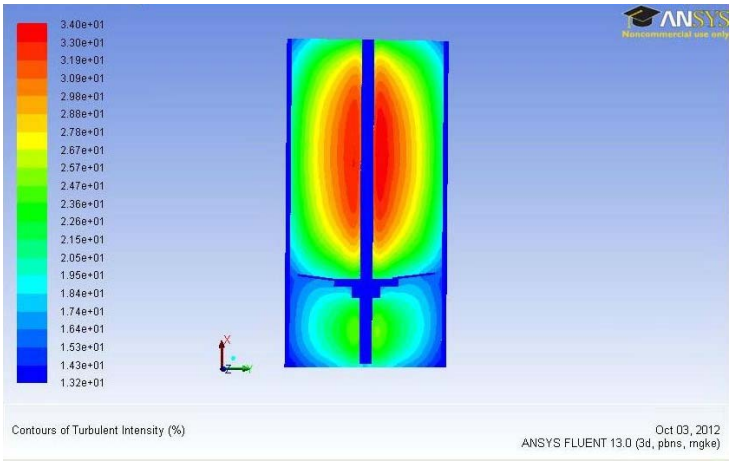
3.40e+01
3.30e+01
3.19e+01
3.09e+01
2.98e+01
2.88e+01
2.78e+01
2.67e+01
2.57e+01
2.47e+01
2.36e+01
2.26e+01
2.15e+01
2.05e+01
1.95e+01
1.84e+01
1.74e+01
1.64e+01
1.53e+01
1.43e+01
1.32e+01
Contours of Turbulent Intensity (%)
Oct 03, 2012
ANSYS FLUENT 13.0 (3d, pbns, mgke)

(b)

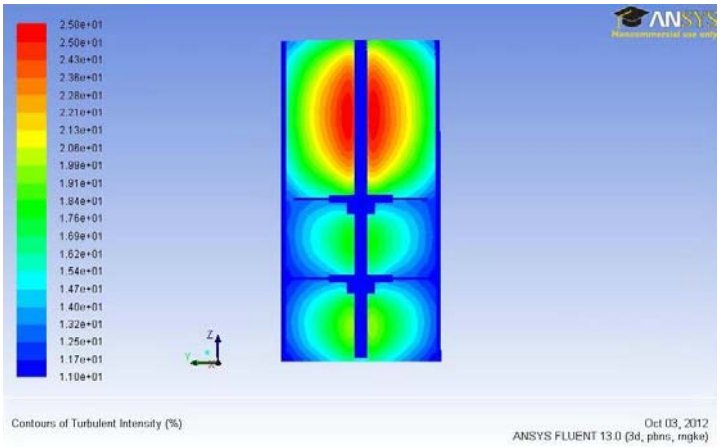
2.50e+01
2.50e+01
2.43e+01
2.36e+01
2.28e+01
2.21e+01
2.13e+01
2.06e+01
1.99e+01
1.91e+01
1.84e+01
1.76e+01
1.69e+01
1.62e+01
1.54e+01
1.47e+01
1.40e+01
1.32e+01
1.25e+01
1.17e+01
1.10e+01
Contours of Turbulent Intensity (%)
Oct 03, 2012
ANSYS FLUENT 13.0 (3d, pbns, mgke)

(c)

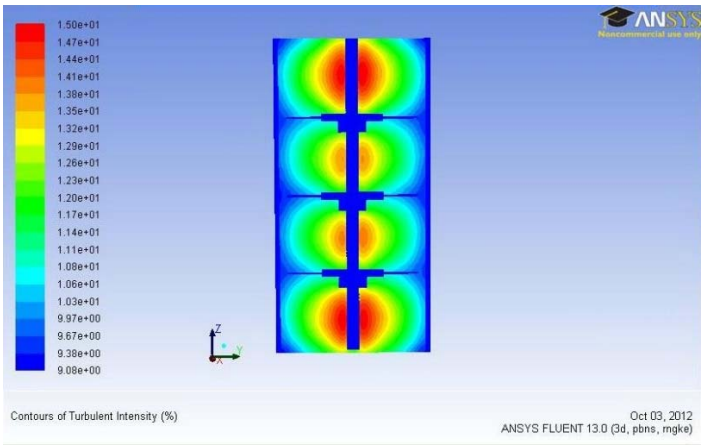
1.50e+01
1.47e+01
1.44e+01
1.41e+01
1.38e+01
1.35e+01
1.32e+01
1.29e+01
1.26e+01
1.23e+01
1.20e+01
1.17e+01
1.14e+01
1.11e+01
1.08e+01
1.06e+01
1.03e+01
9.97e+00
9.67e+00
9.38e+00
9.08e+00
Contours of Turbulent Intensity (%)
Oct 03, 2012
ANSYS FLUENT 13.0 (3d, pbns, mgke)

Figure 2. Flow field simulation in the photocatalytic impeller reactor comparing different numbers of impellers.

The reactor has an illuminated catalyst surface area per unit reactor volume of 17.57 m^{-1} which is a lower limit of the real value due to the porous morphology of the immobilized TiO_2. The diffusion flux of the toluene vapour through the thin-film simultaneously with photocatalytic degradation of gaseous molecules is described by equation (1)[22]:

$$\frac{\delta_q}{\delta_t} = D_s\left(\frac{\delta^2 q}{\delta z^2}\right) - kI^m q^n \qquad (1)$$

where q is the concentration of sorbed gaseous molecules in the thin-film catalyst, D_s is the effective diffusivity, in the catalyst, k is the photocatalytic reaction rate constant, I is the illumination intensity, z is the distance from the catalyst support surface, t is the reaction time while m and n are constants of reaction order. The first term on the right hand side accounts for internal mass transfer and is a product of toluene diffusivity in air (D_s = 8.7E-6 m^2/s) and Fick's second law of diffusion. The second term accounts for the photocatalytic reaction taking place.

3.2 Toluene vapour degradation

Known volume of toluene vapour (Fisher scientific) was withdrawn from toluene reagent headspace at room temperature of 23 °C using a gas tight syringe (SGE), and introduced into the air saturated reactor. The starting concentrations in the reactor were normalised from ppm to 100% hence, the amount of toluene vapour left in the reactor could be determined. This ensured any slight variations in starting concentration of the known volume of toluene were taken into consideration when monitoring toluene mineralisation. Control measurements of toluene vapour concentration in the reactor were taken over a period of 1 h without UV illumination and immobilized catalyst, with immobilized catalysts alone and with UV illumination alone. The proximity of the source of UV illumination to the reactor, increased the treatment temperature within the reactor. This aided the diffusion and desorption of toluene from the immobilised catalyst surface. The toluene concentration sampling device detected this as an

initial increase in concentration (fig. 3). Photocatalytic degradation of toluene involved illumination of the immobilized catalysts by a UV LED array of 5.58 Wm^{-2} intensity immediately after 10 mins of dark adsorption. This was followed by the rotation of the photocatalytic modified Rushton impellers at 10 rev/min and real-time monitoring of toluene concentration with a VOC monitor (MiniRAE 2000).

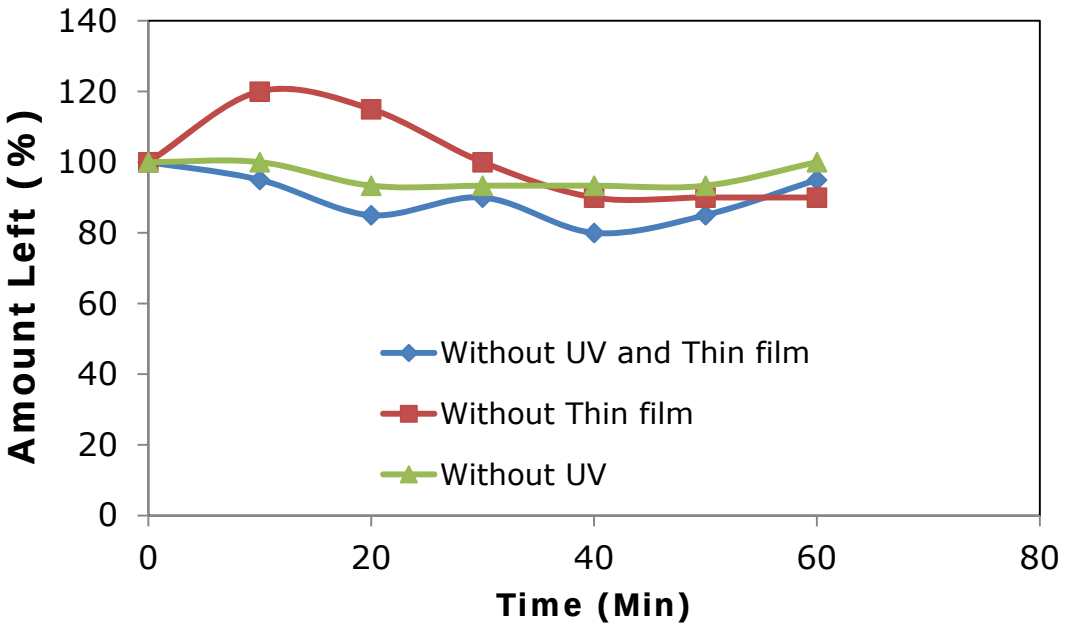

Figure 3. Control experiments in the PIR reactor showing effect of UV illumination on toluene concentration.

3.3 Characterization of immobilized TiO_2

Chemical characterization of the immobilized TiO_2 thin-film was carried out using the energy-dispersive X-ray spectroscopy (EDX) to determine the chemical composition of the thin-film while surface and thickness were characterized with a scanning electron microscope (SEM). The SEM micrographs reveal a continuous film of TiO_2 having a thickness of 8 μm. EDX spectra and SEM micrographs of the TiO_2 coating are shown in figure 4. Chang et al.[36] studied the effect of immobilized TiO_2 thickness on pollutant degradation and experimentally determined the optimum thickness for thin-film catalysts to be between 2 μm – 8 μm. At a greater thickness, charge carriers travel longer distances to active sites[37].

Synthesis and characterisation of TiO_2 thin films have been widely reported in the literature[14-17]. The basic properties of a simple immobilised catalyst film, on the modified Rushton impellers in the PIR reactor configuration is sufficient in eliminating mass transfer limitations. EDX spectra confirmed the presence of TiO_2 in the elemental composition of the synthesized thin film. Scanning electron microscopy (SEM) was used to determine the thickness of the thin film coating on the glass substrate.

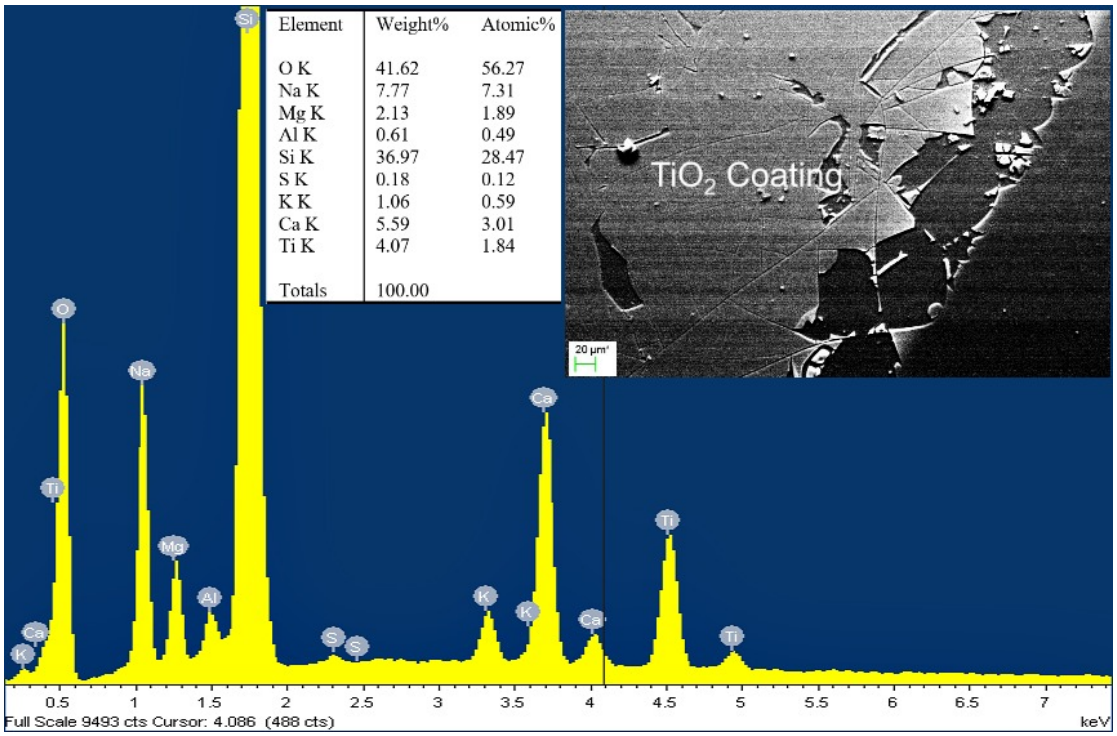

Figure 4. EDX spectra showing the presence of the elements Ti and O (inset: table of elemental composition and SEM micrograph).

The absorbance of the thin-film was characterized using UV-Vis spectroscopy (Perkin Elmer Lambda950); absorbance of photons is a required step for charge separation which leads to the generation of electron-hole pairs that are responsible for the photocatalytic process. The glass slides which have no UV absorbance at the emitting wavelength of the UV LEDs (360 nm) showed significant UV absorbance after TiO_2 immobilization (fig. 5). The emission wavelength of the UV-Vis spectrophotometer lamp in nm is shown on the horizonal axis with the corresponding absorbance by the immobilised TiO_2 film on the vertical axis.

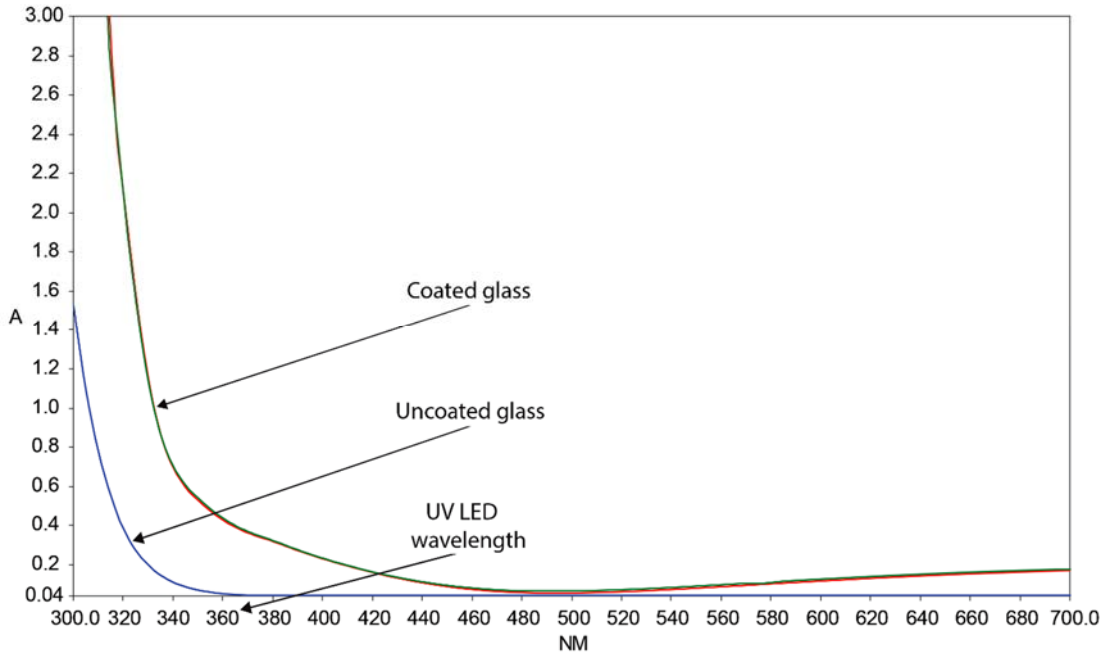

Figure 5. UV absorbance spectra of glass slide before and after TiO_2 immobilization.

4. Discussion

4.1 Toluene photo-oxidation in the PIR reactor

The stoichiometry and reaction pathway of complete mineralization of toluene by TiO_2 photocatalysis has been widely studied and reported[38,39]. Due to the low illuminated catalyst surface area per unit reactor volume compared to reactors of other configurations[40], toluene degradation rate proceeded moderately with around 50% degradation achieved after a reaction time of 3 hours. The average degradation rate is determined for the reaction due to the long reaction times. It is obtained by taking the change in toluene vapour concentration over a time period. Upon UV illumination, adsorbed toluene molecules desorb from the surface resulting in an increase in measured concentration. This is followed by a steady rate of degradation which later declines as a result of gradual loss of activity of the immobilized TiO_2 catalyst, film due to strong binding of intermediate species on the catalyst surface[41].

The reaction pathway of toluene photo-oxidation involves the formation of different solid aromatic intermediates which compete with toluene

molecules for surface area on the immobilised catalyst. This leads to catalyst deactivation. The strongly bound solid intermediates formed during toluene photo-oxidation have been previously identified by Ardizzone *et al.*[41] as benzoic acid, benzaldehyde and benzyl alcohol. Unlike single-pass reactors, catalyst deactivation in batch reactors is concealed by the concentration gradients in the reactor over the reaction time. Regeneration of the deactivated catalyst has been reported in the literature through simple water treatment or UV illumination in fresh air flow[27,41]. The presence of water vapour enhances complete mineralisation of toluene however, toluene photo-oxidation in the PIR reactor was carried out in the absence of water vapour. This greatly affected the performance of the immobilised TiO_2 catalyst as it was continuously deactivated. The effect of deactivation on toluene photo- oxidation was investigated by carrying out repeated runs of the same experimental conditions using the same photocatalytic impeller after flushing the reactor with fresh air. Reduced activity of the TiO_2 catalyst film becomes evident after the second run with almost total loss of activity on the fourth run.

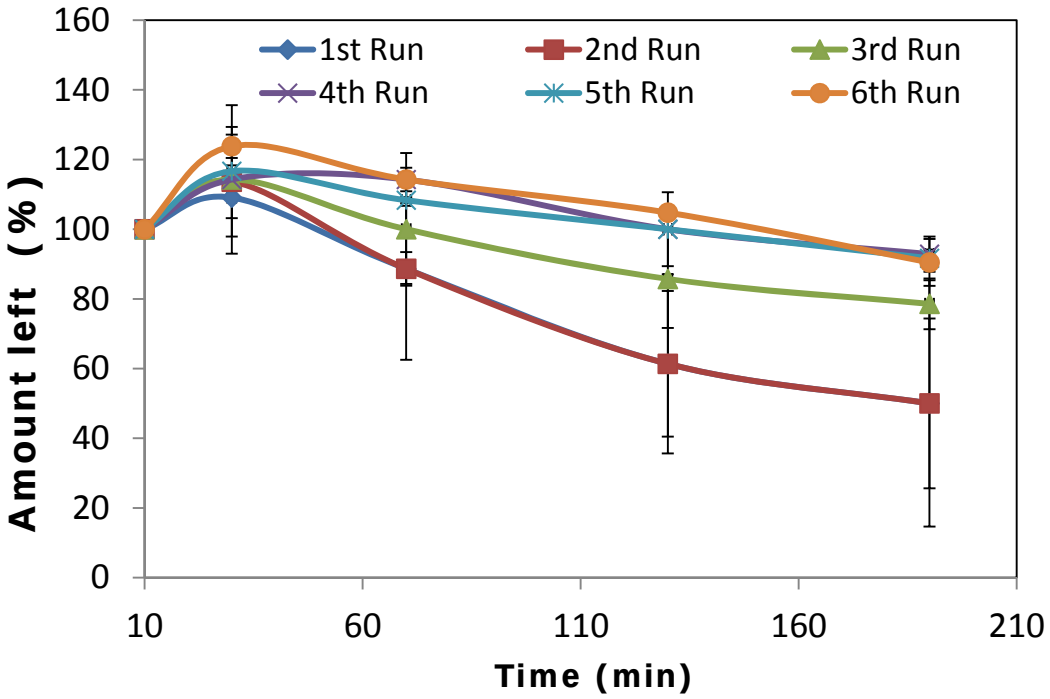

Figure 6. Photo-oxidation of toluene vapour showing loss of catalyst activity with repeated runs. The error bars are the standard deviations from the mean value of repeated experiments.

4.2 Langmuir-Hinshelwood kinetics

The rate of gas phase photo-oxidation of several VOCs including toluene have been previously shown to obey the Langmuir-Hinshelwood rate equation[42](2), the accuracy of this model is based on the adsorption of a single reactant to the surface and the assumption that there is little or no competing adsorption by intermediate products.

$$-r = \frac{kK_{ads}[Toluene]}{1 + K_{ads}[Toluene]} \qquad (2)$$

At the low concentrations used in this study, between 2 ppm and 11 ppm, adsorption of toluene onto the photocatalytic impellers was marginal, reduced activity due to deactivation was noticeable after the first 6 hours. First-order kinetics was observed for the disappearance of toluene within this concentration and a linear plot of the double reciprocal of rate versus concentration verified the suitability of the Langmuir-Hinshelwood rate equation in modelling the photocatalytic reaction rates (fig. 7) with calculated apparent rate constant k of 0.0118 s^{-1} and a Langmuir adsorption coefficient K_{ads} of 0.3316 dm^3 ppm^{-1}.

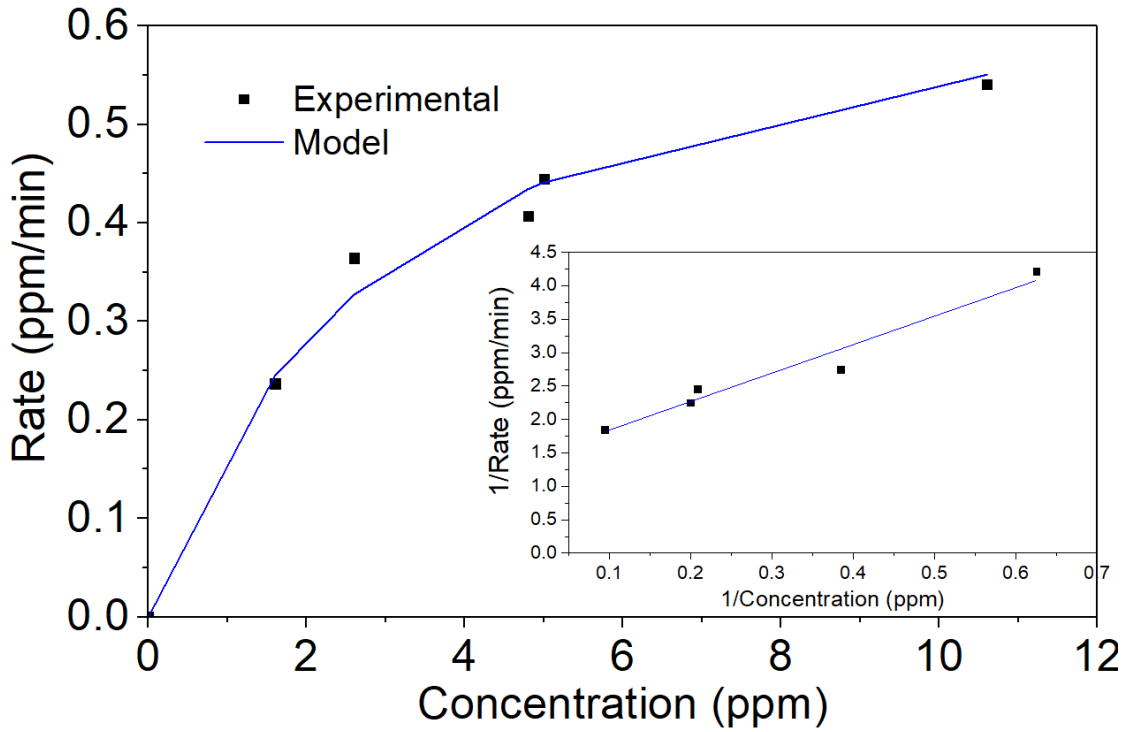

Figure 7. Comparison of toluene experimental and model photo-oxidation rates. (Inset: double reciprocal plot of rate versus concentration).

4.3 Influence of mass transfer

The first-order heterogeneous photocatalytic degradation of the toluene vapour occurs at the boundary of the diffusion domain and is therefore possibly diffusion limited. For photocatalytic reactions that obey the Langmuir-Hinshelwood rate equation, the heterogeneous second Damköhler number[43](3) is a representation of the ratio of the heterogeneous reaction rate to the radial diffusion rate. A Damköhler number above unity indicates toluene diffusion time scale is greater than toluene reaction time scale hence, the overall process is mass transfer limited and vice versa.

$$\mathrm{Da_{II}} = \frac{\text{Reaction rate}}{\text{Diffusive mass transport}} \qquad (3)$$

For the reactor used in this study which is characterized by a radial flow aided by the impellers within the reactor, the dimensionless second Damköhler number was derived using the equation adapted by Gorges *et al.*[44] as follows:

$$\mathrm{Da_{II}} = \frac{k}{\left[\left(\frac{\beta a}{K_{ads}}\right) + \beta a C_b\right]} \qquad (4)$$

Where k is the apparent rate constant, K_{ads} is the Langmuir adsorption coefficient obtained from the slope of the double reciprocal linear plot in figure 8 where $1/k$ is the intercept and $1/k\,K_{ads}$ equals the slope, C_b is the bulk toluene concentration, a is the interfacial area per unit volume of the reactor while β is the mass transfer coefficient such that;

$$Sh \equiv \frac{\beta dh}{D_s} \qquad (5)$$

dh and D_s are the reactor hydraulic diameter (0.094 m) and diffusivity of toluene in air respectively, Sh is the Sherwood number computed from Froessling equation (6)

$$Sh = 2 + 0.55Re^{0.5}Sc^{0.3} \quad (6)$$

Where Re and Sc are the dimensionless Reynolds (1.418) and Schmidt (17) numbers respectively. Table 1. shows the Damköhler number at different bulk concentrations, the results shows $Da_{II} < 1$ for all bulk concentrations indicating toluene photo-oxidation within the PIR reactor is reaction controlled. An increase in Da_{II} as bulk concentration decreases is observed, this is consistent with previous studies[44] and Fick's first law hence, mass transfer limitations are greater at lower bulk concentrations of toluene photo-oxidation in the reactor.

Table 1. Damköhler number of toluene degradation at different bulk concentrations

C_b (ppm)	Damköhler no. (Da_{II})
10.6	0.2
5.0	0.3
4.8	0.3
2.6	0.4
1.6	0.4

4.4 Photonic efficiency of the photocatalytic reaction

In gas phase heterogeneous photocatalysis, typical quantum yields (φ) for reactions involving TiO_2 catalysts may exceed 50% under low UV illumination[45]. This low efficiency has been previously attributed to mass transfer limitations, slow oxygen scavenging and charge-carrier recombination[46-48]. For toluene photo-oxidation in the PIR reactor, photonic efficiency (ζ) (7) which takes into consideration the photons incident on the photocatalyst and is therefore a lower limit of φ was correlated with mass transfer limitation and catalyst deactivation through the Damköhler number and reduced rates of reaction through loss of catalyst activity respectively (Table 2.).

$$\zeta = \frac{\text{Reaction rate}}{\text{Incident photon rate}} \qquad (7)$$

Table 2. Reducing photonic efficiency of toluene photo-oxidation

C_b (ppm)	Rate (ppm/s)	Photonic Efficiency (%)	Da_{II}
4.4	2.04E-04	2.0	0.3
4.4	2.04E-04	2.0	0.3
1.4	2.78E-05	0.3	0.5
1.4	9.26E-06	0.1	0.5
1.2	9.26E-06	0.1	0.5

Incident photon rate for our UV-LED array was 9.98E-7 Einsteins L^{-1} s^{-1}, the reaction rates for toluene photo-oxidation were determined using the same photocatalytic impellers for five different 3 hour experiments. The immobilized catalyst deactivated with each experiment and was re-used for subsequent experiments. Different bulk concentrations were used to vary the diffusion flux of toluene. The efficiency of photon utilization during toluene photo-oxidation in the PIR reactor showed a steady reduction as reaction rate reduced due to severe catalyst deactivation with increasing Da_{II} values. This indicates diffusional resistance also contributes to the low photonic efficiencies. The observed photonic efficiency showed equivalent values at both experiments of C_b = 4.4 ppm because the effects of deactivation becomes significant after the first 6 hours. At C_b = 1.4 ppm, toluene photo-oxidation rate is slower for the latter experiment hence, a lower photonic efficiency. After 12 hours of continuous toluene photo-oxidation, the immobilized catalyst is deactivated and this is indicated by the stagnating photo-oxidation rates and photonic efficiency at C_b = 1.4 ppm and 1.2 ppm.

5. Conclusion

In gas-solid heterogeneous photocatalysis, mass transfer of the reactants from the bulk to the catalyst surface is the single most important

step. This is especially important in the photo-oxidation of VOCs which deactivate TiO_2 catalysts when solid intermediates are formed. Ultimately, the efficiency of photon utilization during the photo-oxidation of toluene is a function of the reaction rate. This is affected by any limitations in mass diffusion of toluene to the immobilized catalyst and the simultaneous deactivation process. For the reactor used in this study, toluene photo-oxidation was reaction limited even prior to the deactivation of the immobilized catalyst. The PIR reactor configuration is therefore characterised and limited by slow reaction rates, hence increasing the total surface area of the immobilised catalyst through larger or more impellers is recommended for PIR reactor configurations. In the treatment of pollutants which form solid intermediates, deactivation of the catalyst decreases treatment efficiency. The primary concern in the design of future PIR reactors or reactors of similar design will be overcoming these limitations or adequately accounting for their effects. Further work on standardising the photocatalytic impeller reactor are currently ongoing.

Acknowledgement

The authors would like to thank the Scottish Funding Council who funded R. Prabhu's lectureship through the Northern Research Partnership's research pooling initiative in engineering.

REFERENCES

(1) Andreozzi, R.; Caprio, V.; Insola, A.; Marotta, R. Advanced Oxidation Processes (AOP) for Water Purification and Recovery. *Catalysis Today* **1999***, 53*, 51-59.

(2) Tokode, O.; Prabhu, R.; Lawton, L. A.; Robertson, P. K. Controlled periodic illumination in semiconductor photocatalysis. *Journal of photochemistry and photobiology A: chemistry* **2016**, 319, 96-106.

(3) Hunger, M.; Hüsken, G.; Brouwers, H. Photocatalytic Degradation of Air pollutants—From Modeling to Large Scale Application. *Cem. Concr. Res.* **2010***, 40*, 313-320.

(4) Chen, X.; Shen, S.; Guo, L.; Mao, S. S. Semiconductor-Based Photocatalytic Hydrogen Generation. *Chem. Rev.* **2010***, 110*, 6503-6570.

(5) Park, H.; Kim, K. Y.; Choi, W. A Novel Photoelectrochemical Method of Metal Corrosion Prevention using a TiO_2 Solar Panel. *Chemical Communications* **2001**, 281-282.

(6) Ollis, D., Ed.; In *Photocatalytic Treatment of Water: Irradiance Influences, in Photocatalysis and Water Purification: From Fundamentals to Recent Applications (ed P. Pichat);* Wiley-VCH Verlag GmbH & Co. KGaA, Weinheim, Germany.: Weinheim, Germany, **2013**, pp 311-333.

(7) Bahnemann, D.; Bockelmann, D.; Goslich, R. Mechanistic Studies of Water Detoxification in Illuminated TiO_2 Suspensions. *Solar Energy Materials* **1991***, 24*, 564-583.

(8) Tokode, O.I.; Prabhu, R.; Lawton, L.A.; Robertson, P.K. Effect of controlled periodic-based illumination on the photonic efficiency of photocatalytic degradation of methyl orange. *Journal of catalysis* **2012,** 290, 138-142.

(9) Tokode, O.I.; Prabhu, R.; Lawton, L.A.; Robertson, P.K. The effect of pH on the photonic efficiency of the destruction of methyl orange under controlled periodic illumination with UV-LED sources. *Chemical Engineering Journal* **2014**, 246, 337-342.

(10) Hoffmann, M.R; Martin, S. T; Choi, W.; Bahnemann, D. W. Environmental Applications of Semiconductor Photocatalysis. *Chem. Rev.* **1995***, 95*, 69-96.

(11) Tokode, O. Photocatalytic destruction of volatile organic compounds from the oil and gas industry. *Robert Gordon University PhD Thesis* **2014**.

(12) Tokode, O.I.; Prabhu, R.; Lawton, L.A.; Robertson, P.K. Mathematical modelling of quantum yield enhancements of methyl orange photooxidation in aqueous TiO_2 suspensions under controlled periodic UV LED illumination. *Applied catalysis B: environmental* **2014**, 156, 398-403.

(13) Mills, A.; Le Hunte, S. An Overview of Semiconductor Photocatalysis. *J. Photochem. Photobiol. A.* **1997***, 108*, 1-35.

(14) Reddy, K.R.; Karthik, K.V.; Prasad, S.B.; Soni, S.K.; Jeong, H.M.; Raghu, A.V. Enhanced photocatalytic activity of nanostructured titanium dioxide/polyaniline hybrid photocatalysts. *Polyhedron* **2016**, 120, 169-174.

(15) Reddy, K.R.; Nakata, K.; Ochiai, T.; Murakami, T.; Tryk, D.A.; Fujishima, A. Facile fabrication and photocatalytic application of Ag nanoparticles-TiO2 nanofiber composites. *Journal of nanoscience and nanotechnology* **2011**, 11(4), 3692-3695.

(16) Reddy, K.R.; Nakata, K.; Ochiai, T.; Murakami, T.; Tryk, D.A.; Fujishima, A. Nanofibrous TiO_2-core/conjugated polymer-sheath composites: synthesis, structural properties and photocatalytic activity. *Journal of nanoscience and nanotechnology* **2010**, 10(12), 7951-7957.

(17) Mazierski, P.; Malankowska, A.; Kobylański, M.; Diak, M.; Kozak, M.; Winiarski, M.J.; Klimczuk, T.; Lisowski, W.; Nowaczyk, G.; Zaleska-Medynska, A. Photocatalytically active TiO_2/Ag_2O nanotube arrays interlaced with silver nanoparticles obtained from the one-step anodic oxidation of Ti–Ag alloys. *ACS Catalysis* **2017**, 7(4), 2753-2764.

(18) McCullagh, C.; Skillen, N.; Adams, M.; Robertson, P. K. J. Photocatalytic Reactors for Environmental Remediation: A Review. *Journal of Chemical Technology & Biotechnology* **2011***, 86*, 1002-1017.

(19) Bouchy, M.; Zahraa, O. Photocatalytic Reactors. *International Journal of Photoenergy* **2003***, 5*, 191-197.

(20) Cassano, E. A.; Martin, A. C.; Brandi, J. R.; Alfano, M. O. Photoreactor Analysis and Design: Fundamentals and Applications. *Ind. Eng. Chem. Res.* **1995***, 34*, 2155-2201.

(21) Tokode, O.I.; Prabhu, R.; Lawton, L.A.; Robertson, P.K. UV LED sources for heterogeneous photocatalysis. In *Environmental Photochemistry Part III* **2014**, (pp. 159-179). Springer Berlin Heidelberg.

(22) Shan, A. Y.; Ghazi, T. I. M.; Rashid, S. A. Immobilisation of Titanium Dioxide onto Supporting Materials in Heterogeneous Photocatalysis: A Review. *Applied Catalysis A: General* **2010***, 389*, 1-8.

(23) Cassano, A. E.; Alfano, O. M. Reaction Engineering of Suspended Solid Heterogeneous Photocatalytic Reactors. *Catalysis Today* **2000***, 58*, 167-197.

(24) Liou, P.; Chen, S.; Wu, J. C.; Liu, D.; Mackintosh, S.; Maroto-Valer, M.; Linforth, R. Photocatalytic CO2 Reduction using an Internally Illuminated Monolith Photoreactor. *Energy & Environmental Science* **2011***, 4*, 1487-1494.

(25) Sauer, M. L.; Hale, M. A.; Ollis, D. F. Heterogenous Photocatalytic Oxidation of Dilute Toluene-Chlorocarbon Mixtures in Air. *J. Photochem. Photobiol. A.* **1995***, 88*, 169-178.

(26) Paschoalino, M.; Jardim, W. Indoor Air Disinfection using a Polyester Supported TiO_2 photo-reactor. *Indoor Air* **2008***, 18*, 473-479.

(27) Prieto, O.; Fermoso, J.; Irusta, R. Photocatalytic Degradation of Toluene in Air using a Fluidized Bed Photoreactor. *International Journal of Photoenergy* **2007**.

(28) Li Puma, G.; Yue, P.L. Comparison of the effectiveness of photon-based oxidation processes in a pilot falling film photoreactor. *Environmental science & technology*. **1999,** 33(18), 3210-3216.

(29) Adams, M.; Campbell, I.; Robertson, P.K. Novel photocatalytic reactor development for removal of hydrocarbons from water. *International Journal of Photoenergy* **2008**.

(30) Martin, S.T.; Herrmann, H.; Hoffmann, M.R. Time-resolved microwave conductivity. *J. Chem. Soc. Faraday Trans* **1994,** 90(21), 3323-3330.

(31) Kuo, H.P.; Wu, C.T.; Hsu, R.C. Continuous reduction of toluene vapours from the contaminated gas stream in a fluidised bed photoreactor. *Powder Technology* **2009,** 195(1), 50-56.

(32) Peill, N. J.; Hoffmann, M. R. Development and Optimization of a TiO_2-Coated Fiber-Optic Cable Reactor: Photocatalytic Degradation of 4-Chlorophenol. *Environ. Sci. Technol.* **1995***, 29*, 2974-2981.

(33) Ray, A. K.; Beenackers, A. A. Development of a New Photocatalytic Reactor for Water Purification. *Catalysis Today* **1998***, 40*, 73-83.

(34) Alphonse, P.; Varghese, A.; Tendero, C. Stable Hydrosols for TiO_2 Coatings. *J. Sol-Gel Sci. Technol.* **2010***, 56*, 250-263.

(35) Turchi, C. S.; Ollis, D. F. Comment. Photocatalytic Reactor Design: An Example of Mass-Transfer Limitations with an Immobilized Catalyst. *J. Phys. Chem.* **1988***, 92*, 6852-6853.

(36) Chang, H. T.; Wu, N.; Zhu, F. A Kinetic Model for Photocatalytic Degradation of Organic Contaminants in a Thin-Film TiO_2 Catalyst. *Water Res.* **2000***, 34*, 407-416.

(37) Tennakone, K.; Tilakaratne, C. T. K.; Kottegoda, I. R. M. Photomineralization of Carbofuran by TiO_2-Supported Catalyst. *Water Res.* **1997***, 31*, 1909-1912.

(38) d'Hennezel, O.; Pichat, P.; Ollis, D. F. Benzene and Toluene Gas-Phase Photocatalytic Degradation Over H_2O and HCL Pretreated TiO_2: By-Products and Mechanisms. *J. Photochem. Photobiol. A.* **1998***, 118*, 197-204.

(39) Bianchi, C. L.; Gatto, S.; Pirola, C.; Naldoni, A.; Di Michele, A.; Cerrato, G.; Crocellà, V.; Capucci, V. Photocatalytic Degradation of Acetone, Acetaldehyde and Toluene in Gas-Phase: Comparison between Nano and Micro-Sized TiO_2. *Applied Catalysis B: Environmental* **2014**, *146*, 123-130.

(40) Ray, A. K.; Beenackers, A. A. Novel Photocatalytic Reactor for Water Purification. *AIChE J.* **1998**, *44*, 477-483.

(41) Ardizzone, S.; Bianchi, C.; Cappelletti, G.; Naldoni, A.; Pirola, C. Photocatalytic Degradation of Toluene in the Gas Phase: Relationship between Surface Species and Catalyst Features. *Environ. Sci. Technol.* **2008**, *42*, 6671-6676.

(42) Boulamanti, A. K.; Korologos, C. A.; Philippopoulos, C. J. The Rate of Photocatalytic Oxidation of Aromatic Volatile Organic Compounds in the Gas-Phase. *Atmos. Environ.* **2008**, *42*, 7844-7850.

(43) Clark, M. M. In *Transport modeling for environmental engineers and scientists;* John Wiley & Sons: **2012**.

(44) Gorges, R.; Meyer, S.; Kreisel, G. Photocatalysis in Microreactors. *J. Photochem. Photobiol. A.* **2004**, *167*, 95-99.

(45) Cornu, J. G. C.; Colussi, A. J.; Hoffmann, R. M. Quantum Yields of the Photocatalytic Oxidation of Formate in Aqueous TiO_2 Suspensions Under Continuous and Periodic Illumination. *J. Phys. Chem. B* **2001**, *105*, 1351-1354.

(46) Lewis, N. S. Progress in Understanding Electron-Transfer Reactions at semiconductor/liquid Interfaces. *The Journal of Physical Chemistry B* **1998**, *102*, 4843-4855.

(47) Ollis, D. F.; Al-Ekabi, H., Eds. In *Photocatalytic Purification and Treatment of Water and Air;* Hussain Al-Ekabi, Ed.; Elsevier: New York, USA, **1993**, pp 820.

(48) Upadhya, S.; Ollis, D. F. Simple Photocatalysis Model for Photoefficiency Enhancement Via Controlled, Periodic Illumination. *J. Phys. Chem. B* **1997**, *101*, 2625-2631.